

Observation of Envelope Solitons in Solids

J. Wu,^(a) J. Wheatley,^(b) S. Putterman, and I. Rudnick

Physics Department, University of California, Los Angeles, California 90024

(Received 4 September 1987)

We have observed highly nonlinear localized wave packets propagating as flexural modes of thin shells. They maintain their structure in a collision and have envelopes in quantitative agreement with the soliton solutions to the nonlinear Schrödinger equation.

PACS numbers: 43.25.+y, 62.30.+d

Since the first observation in 1834 of a soliton in a canal,¹ the potential importance of coherent long-lived localized states of continuous media driven far off equilibrium has received considerable attention.¹⁻⁴ Solitons appear to be physically favored in one-dimensional systems, though they have been predicted in two-dimensional systems.^{2,5} Linearly stable solitary waves have been derived from the Gross-Pitaevskii equation in three dimensions.⁶ Apart from observations in the Andaman sea,⁷ naturally occurring solitons have eluded observation, but they have been predicted to play a role in biological systems such as macromolecules which are largely one dimensional.⁸ In this paper we report the observation of the formation of envelope-type solitons in an elastic medium.

Part of the motivation for this work finds its origin in the mechanics of "natural engines."⁹ In this regard, our goal is to determine whether the spontaneous symmetry breaking which leads to soliton formation would eliminate the need for the externally imposed "broken thermodynamic symmetry," such as is realized with the stack of plates in the acoustic engine. In addition, could

a macroscopic soliton act as a means of focusing heat as well as mechanical energy? Another important goal is the generation of nonpropagating solitons¹⁰ in elastic media.

The elastic medium in which we set out to search for soliton behavior is a seamless, open-ended, nickel, cylindrical, thin (0.009 cm) shell made by an electroplating process and having dimensions shown in Fig. 1. In order to approximate fixed-boundary conditions, the top and bottom rims are thick (0.028 cm) compared with the shell thickness. The shell is supported by six pairs of monofilament nylon threads under almost vertical tension. The shell is excited by an acoustic beam generated by a horn driver with a mouth area of 20 cm², coupled to a horn whose cross-sectional area decreases exponentially to about 3 cm². This means of transduction is found to be superior to direct electrostatic or electromagnetic forcing of the shell. The elastic waves so generated in the shell are flexural in character and have both an axial x and circumferential y component; p and q are the corresponding modal eigennumbers.

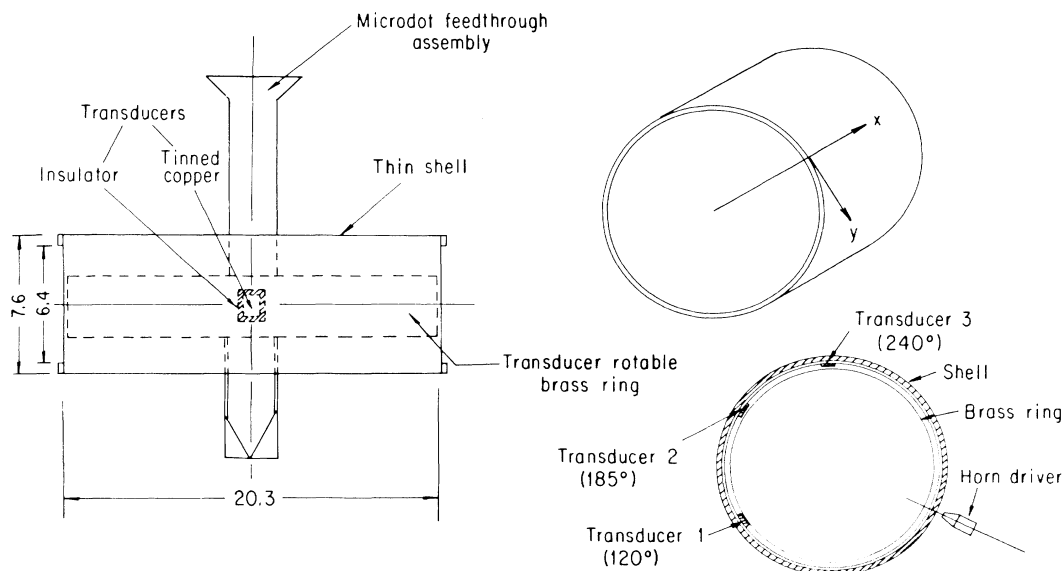


FIG. 1. Experimental arrangement.

Our reason for studying thin shells is that this system has a huge dispersion, large quality factor Q , and high nonlinear response. Such a combination of parameters generally makes structure formation (e.g., solitons) in off-equilibrium systems accessible to observation.

The reversible dispersion, which is due to a nonlinear dependence of frequency on wave number, is apparent from the measured spectrum of small-amplitude vibration shown in Fig. 2. We have investigated modes in which p is always 1 and q ranges from 6 to 32. The only modes which we failed to excite (for unknown reasons) were $q = 9, 10, \text{ and } 19$. The minimum in the spectrum is interesting in its own right (note some similarity with the roton minimum in superfluid helium), and for a uniform shell the dispersion law is calculated to be¹¹

$$\omega_{p,q}^2 = \frac{E}{\rho R^2} \left(\frac{\xi^4}{(\xi^2+1)^2} + \frac{\epsilon(\xi^2+1)^2}{12(1-\nu^2)} \right), \quad (1)$$

where $\xi = \pi R p / L q$, $\epsilon = q^4 h^2 / R^2$, and ρ is the volume density of the material, E is Young's modulus, ν is Poisson's ratio, L is the height, R the radius, and h the thickness of the shell. The solid line in Fig. 2 is a plot of Eq. (1) for this shell; $\omega = 2\pi f$, where f is the frequency.

The amplitude-dependent nonlinear response of the shell is determined from the shift df in the resonant frequency of the mode $p=1, q=23$, as a function of the shell's flexural displacement amplitude z . The measured shift is given by

$$df/f = \gamma z^2/h^2, \quad (2)$$

where $\gamma = -23$.

To measure z we used capacitive transducers mounted on a brass ring (Fig. 1). The ring is coaxial with the shell and can be rotated about the axis. The transducers are used to probe the radial displacement of the flexural modes. Another single, similar transducer can be moved along the axial direction in order to measure displace-

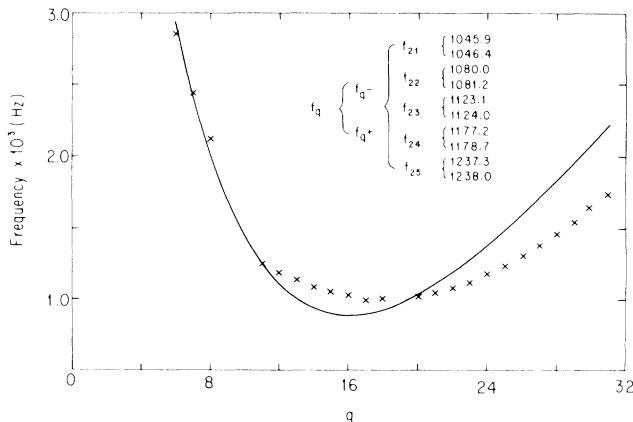


FIG. 2. Dispersion law for the $(1,q)$ modes; the crosses are experimental data.

ment as a function of height along the shell. The transducers were independently calibrated with a B&K vibration exciter and accelerometers. They are still linear to within 5% at amplitudes that exceed by a factor of 10 the largest amplitudes reported herein. The conversion factor from voltage output to displacement amplitude is 1.60×10^{-5} cm/mV. The maximum amplitude achieved near 1120 Hz is 2×10^{-4} cm, which corresponds to a Mach number of about 10^{-4} . At these amplitudes the frequency shift due to nonlinearity is approximately 5 times the bandwidth due to attenuation, the Q being about 500.

In a typical experiment, a flexural wave pulse is generated by our blasting the shell with an acoustic wave train that is five waves long. In Fig. 3 the top curve is the wave pulse at 1120 Hz applied to the horn-driven unit. The three oscilloscope traces shown in Fig. 3 give the response of the shell at $120^\circ, 185^\circ, \text{ and } 240^\circ$ (see Fig. 1) relative to the drive. Note the two localized packets clearly visible at 240° and 120° in Fig. 3. For reasons discussed below, we claim that these packets are envelope solitons. The larger-amplitude packet arrives first at the 120° transducer and is therefore an envelope soliton traveling clockwise (CW) at a velocity found to be 26 m/s. The smaller-amplitude packet arrives first at 240° and later at 120° and is therefore an envelope soli-

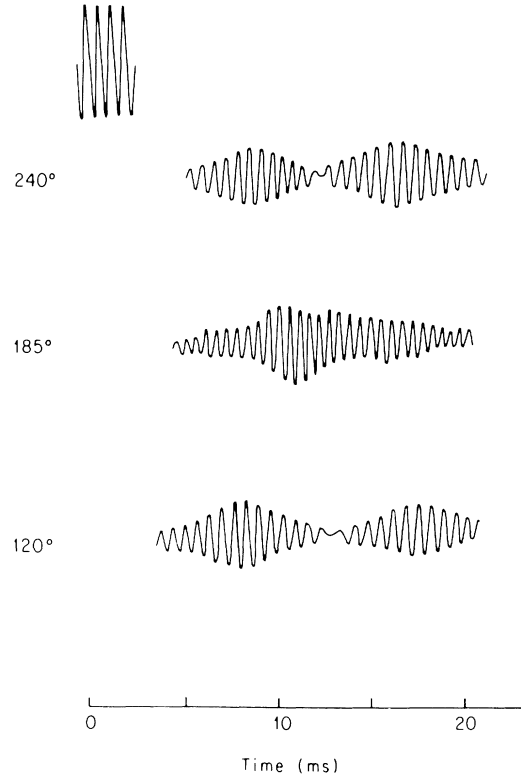


FIG. 3. Collision of CW and CCW envelope solitons as shown by oscilloscope traces.

ton traveling counterclockwise (CCW) at a velocity found to be 23 m/s. The displacement observed at 185° occurs where two wave packets overlap or collide. The solitons emerge unscathed from the collision and furthermore the strong nonlinear nature of this interaction is indicated by the fact that the sum of the amplitudes of the separate solitons is about 25% greater than the maximum amplitude observed at 185° . For small-amplitude (about 2% of those at which solitons form) pulses, the interaction packet is observed to be the sum of the CW and CCW pulses. Even in the linear limit, the apparent group velocities for the CW and CCW packets are different. These velocities are the same as for the CW and CCW solitons. We believe that a given mode q can give rise to different apparent group velocities for CW and CCW motion because of the splitting of CW and CCW degeneracy by effects which break axisymmetry. This splitting (see Fig. 2) is a strong function of mode number. By driving of the shell at a different location, the time-reversed state to Fig. 3 can be easily generated. Our experiments indicate that at the maximum amplitudes of drive available, the most localized packets are obtained by driving of the shell at a location which maximizes the difference in group velocities of clockwise and counterclockwise pulses.

Figure 4 is a plot of the response at the 120° transducer during a time span for which a pulse would travel about four circuits of the shell; A_1 , A_2 , and A_3 refer to successive recordings of the CW soliton/packet, and B_1 , B_2 , and B_3 refer to the CCW soliton/packet. The 30%

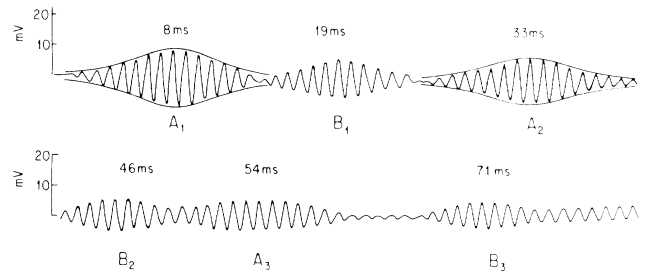


FIG. 4. Temporal response of the shell (as measured at the 120° transducer) to a drive pulse 5 ms long.

attenuation between A_1 and A_3 (or B_1 and B_3) destabilizes the structure and leads to the eventual dispersion of the pulse as indicated. The envelopes drawn through A_1 and A_2 correspond to the best-fit function of

$$\bar{z} = a \operatorname{sech} \alpha (y - v_g t), \quad (3)$$

so that the actual detailed displacement is $z = \bar{z} \cos(k_q y - \omega t)$, where $k_q \equiv q/R$ and for A_1 , $a = 1.7 \times 10^{-4}$ cm, $\alpha = 0.14 \text{ cm}^{-1}$, and $v_g = 26$ m/s, while for A_2 , $a = 1.4 \times 10^{-4}$ cm and $\alpha = 0.13 \text{ cm}^{-1}$; v_g is unchanged. For B_1 , the envelope (not shown) is $a = 1.2 \times 10^{-4}$ cm, $\alpha = 0.17 \text{ cm}^{-1}$. The fact that a cosine cannot fit these packets is apparent from the inflection point near the half width. The hyperbolic secant is characteristic of the stable envelope-soliton solution to the nonlinear Schrödinger equation (NLS),^{2,12} which we write in the following model-independent form:

$$(\omega_q^2 - \omega^2)\bar{z} - \omega_q (d^2 \omega_q / dk^2) (d^2 \bar{z} / dy^2) + 2\omega_q [\delta \omega_q (|\bar{z}|^2)] \bar{z} = 0, \quad (4)$$

where ω is the frequency of the soliton and $\delta \omega_q$ is given by (2). The NLS generally describes slow modulations of quickly varying hyperbolic classical fields (e.g., optical pulses and surface waves). The soliton response results from the balance between dispersion and nonlinear shift in resonance which can take place only when γ and $d^2 \omega_q / dq^2$ have opposite signs which is the case here. The localized solution to (4) then is

$$\bar{z} = h [(\omega^2 - \omega_q^2) / \gamma \omega_q^2]^{1/2} \operatorname{sech} [(\omega_q^2 - \omega^2) / \omega \omega_q'']^{1/2} (x - v_g t) / R, \quad (5)$$

where $\omega_q'' = d^2 \omega_q / dq^2$.

Equations (4) and (5) connect the measured material parameters γ and ω_q to the theoretically predicted stable, localized coherent state. To compare theory (5) with experiment, say, A_1 , we use the frequency of the drive, 1120 Hz, for $\omega/2\pi$. For q we use the nearest, higher mode which is $q = 23$, so that $\omega_q/2\pi = 1124$ Hz. Unlike infinite systems, where the selection of q is determined by the dominant side-band instability, here the finiteness of the shell perimeter determines the particular mode which is localized. These parameters already determine the theoretical value $a = 1.6 \times 10^{-4}$ cm, in excellent agreement with experiment. The theoretical calculation of the soliton width α^{-1} requires $d^2 \omega / dk^2$. Determination of this parameter from Fig. 2 is complicated by the strong dependence of the splitting on mode number. Thus, we chose to obtain this parameter from

the first derivative of the measured clockwise group velocity of small-amplitude pulses. Noting that $d^2 \omega / dk^2 = dv_g / dk$, we obtain the estimate $d^2 \omega / dq^2 = 24 \text{ s}^{-1}$ and thus calculate $\alpha = 0.14 \text{ cm}^{-1}$.

As $\gamma < 0$, the theoretical picture given here implies that soliton formation cannot occur for ω near to but higher than ω_q . By driving the shell at high amplitude at 1124.5 Hz, we could only observe heavily dispersed pulses with no semblance of the stable structures shown in Figs. 3 and 4. Furthermore, the formation of the soliton ($\omega < \omega_q$) is robust as regards variation of the input envelope of length of wave train.

The excellent agreement between theory and experiment (for a and α) as well as the stability against nonlinear collision is our strongest evidence for interpreting

these packets as solitons. This elastic system is obviously quite rich (e.g., the splittings in ω_q and v_g) and the tendency to form solitons suggests the universality of this phenomenon. On the other hand, at the drive amplitudes which were available, we could only observe this effect at $q=23$ which is precisely the mode where $\omega_q/k \approx d\omega_q/dk$.

To the best of our knowledge, this is the first observation of an envelope soliton [i.e., a nontopological soliton] in a solid. Earlier experiments on fluid surface waves have been interpreted in terms of envelope solitons.¹³

A basic difference between incompressible surface waves and the elastic waves reported here are the associated thermal properties. These should prove to be an interesting direction for further investigation.

We wish to thank B. Denardo, R. Keolian, and A. Larraza for valuable comments. The work of one of us (I.R.) was supported by the U. S. Office of Naval Research. The work of two (J.W. and S.P.) was supported respectively by grants from the U. S. Department of Energy, Divisions of Materials Sciences and Engineering and Geoscience (Office of Basic Energy Science). The work of another (J.W.) was supported by all three of these grants.

^(a)Current address: Physics Department, University of Vermont, Burlington, VT 05405.

^(b)Deceased.

¹J. Scott Russell, Br. Assoc. Adv. Sci. Rep. **14**, 311–390 (1845).

²M. J. Ablowitz and H. Segur, *Solitons and the Inverse*

Scattering Transform (Society for Industrial and Applied Mathematics, Philadelphia, 1981).

³A. C. Scott, F. Y. F. Chu, and D. W. McLaughlin, Proc. IEEE **61**, 1443 (1973); *Solitons*, edited by R. K. Bullough and P. J. Caudrey (Springer-Verlag, Berlin, 1980).

⁴R. K. Dodd, J. C. Eilbeck, J. D. Gibbon, and H. C. Morris, *Solitons and the Nonlinear Wave Equation* (Academic, London, 1982).

⁵B. B. Kadomtsev and V. I. Petviashvili, Dokl. Acad. Nauk SSSR **192**, 753 (1970) [Sov. Phys. Dokl. **15**, 539 (1970)]; S. V. Manakov, V. E. Zakharov, L. A. Bordag, A. R. Its, and V. B. Matveev, Phys. Lett. **63A**, 205 (1977).

⁶C. A. Jones, S. J. Putterman, and P. H. Roberts, J. Phys. A **19**, 2991 (1986); C. A. Jones and P. H. Roberts, J. Phys. A **15**, 2599 (1982).

⁷A. R. Osborne and T. L. Burch, in *Topics in Ocean Physics*, International School of Physics "Enrico Fermi," Course 80, edited by A. R. Osborne and P. Malanotte Rizzoli (North-Holland, Amsterdam, 1982).

⁸A. S. Davydov, *Biology and Quantum Mechanics* (Pergamon, Oxford, 1982); P. S. Lomdahl, S. P. Layne, and I. D. Bigio, Los Alamos Sci. No. 10, 2 (1984).

⁹J. Wheatley, T. Hofler, G. W. Swift, and A. Migliori, Am. J. Phys. **53**, 147 (1985), and J. Acoust. Soc. Am. **74**, 153 (1983); G. W. Swift, A. Migliori, T. Hofler, and J. Wheatley, J. Acoust. Soc. Am. **78**, 787 (1985); J. Wheatley and A. Cox, Phys. Today **38**, No. 8, 50 (1985); J. Wheatley, G. W. Swift, and A. Migliori, Los Alamos Sci. No. 14, 1 (1986).

¹⁰J. Wu, R. Keolian, and I. Rudnick, Phys. Rev. Lett. **52**, 1421 (1984); A. Larraza and S. Putterman, Phys. Lett. **103A**, 15 (1984), and J. Fluid Mech. **148**, 443 (1984); J. Miles, J. Fluid Mech. **148**, 450 (1984).

¹¹L. H. Donnell, *Beams, Plates and Shells* (McGraw-Hill, New York, 1979); M. D. Olson, AIAA J. **3**, 1775 (1965).

¹²V. E. Zakharov and P. B. Shabat, Zh. Eksp. Teor. Fiz. **61**, 118 (1972) [Sov. Phys. JETP **34**, 62 (1972)].

¹³H. C. Yuen and B. M. Lake, Phys. Fluids **18**, 956 (1975).